New Mechanism of the Aeroelastic Divergence Onset

Vasily V. Vedeneev*

Lomonosov Moscow State University, 119991, Moscow, Russia

There are two types of aeroelastic instabilities: divergence and flutter. Flutter is an oscillatory loss of stability, whereas transition to divergence occurs at zero frequency; that is, it is a static instability. A general divergence mechanism described in textbooks consists of a decrease of one of the natural frequencies down to zero due to negative aerodynamic stiffness, coalescence with its paired frequency, and (after the coalescence) transformation to one damped and one growing frequency. Most examples of this mechanism use quasi-steady aerodynamics that, at first sight, is suitable for divergence analyses because of its static nature. In this study, it is shown that, when using unsteady aerodynamics (Theodorsen theory), the analytical structure of eigenfrequencies essentially changes; namely, no frequency coalescence occurs but "structural" eigenfrequencies become damped. The divergence mode is not a continuation of a natural mode, but it separates from a continuous spectrum that exists in the aeroelastic system due to the wake behind the wing when unsteady aerodynamics is used but is absent in the quasi-steady case.

Nomenclature

a	=	parameter of the elastic axis location, $x_f/b - 1$
b	=	half of the chord length; $c/2$, m
c	=	chord length, m
e	=	distance from the aerodynamic center to the elastic axis rated to the chord length, $((1/2) + a)/2 = (x_f - c/4)/c$
k	=	reduced frequency, $\omega c/(2V)$
L	=	aerodynamic force per unit length, N/m
$L_z, L_{\dot{z}}, L_\theta, L_{\dot{\theta}}$	=	oscillatory aerodynamic derivatives
M	=	aerodynamic moment per unit length, N
$M_z, M_{\dot{z}}, M_\theta, M_{\dot{\theta}}$	=	oscillatory aerodynamic derivatives
m	=	wing mass per unit area, kg/m^2
Q_b, Q_t	=	generalized aerodynamic forces, N, N · m
q_b	=	generalized coordinate corresponding to bending wing motion, m
q_t	=	generalized coordinate corresponding to torsional wing motion
s	=	wing span, m
V	=	freestream flow speed, m/s
V_{div}	=	divergence speed, m/s
x_f	=	distance from the leading edge to the elastic axis, m
ρ	=	flow density, kg/m^3
ξ_b	=	Laplace transformation of generalized coordinate q_b, m · s
ξ_t	=	Laplace transformation of generalized coordinate q_t, s
ω	=	eigenfrequency, rad/s
$\omega_{b,t}$	=	natural circular frequency (bending and torsional, respectively), rad/s

I. Introduction

IN MOST aeroelasticity textbooks [1–3], divergence and flutter are considered separately: divergence as a static instability, where steady aerodynamics is employed; and flutter as a dynamic instability, where the use of unsteady aerodynamics is crucial for correct flutter prediction. Even when divergence is considered within the framework of a dynamic system, at best, quasi-steady aerodynamics

is used. In this paper, we reanalyze the classical problem of instability of a two-degree-of-freedom (bending and torsional) system by focusing on divergence but using (unlike most of other studies) fully unsteady Theodorsen aerodynamics. We prove that, first, in addition to the spectrum of eigenfrequencies (two paired eigenfrequencies for a two-degree-of-freedom system), there exists a continuous spectrum consisting of monotonically damped frequencies, which originates from the wake behind the oscillating wing. Second, the growing divergence eigenfrequency is not a smooth continuation of a structural natural frequency. Instead, all "structural" frequencies become damped at a postcritical flow velocity, whereas the divergence mode is an additional mode that exists only at postcritical speeds and separates at the divergence speed from the continuous spectrum.

The structure of the paper is as follows. In Sec. II, we introduce a two-degree-of-freedom aeroelastic model used with variations in all textbooks. Section III is devoted to the eigenfrequency analysis in the framework of different simplified aerodynamic formulations that yield a classical divergence mechanism through the interaction of paired eigenmodes. However, slight improvement of the aerodynamics immediately yields an unexpected result, namely, inability of the divergence to originate from a structural natural mode. In Sec. IV, we reanalyze the problem using fully unsteady aerodynamics and confirm this result. We give an analytical proof of nonexistence of the divergence mode at a subcritical flow speed, which therefore cannot be a transformed structural mode. To go deeper into this problem, we give a closed-form solution of the initial-value problem that establishes the connection between the origin of the divergence mode, the continuous spectrum, and the branch cut of the Theodorsen function. In Sec. V, we compare the present results with previous studies that used various numerical methods. Finally, in Sec. VI, we summarize the results and discuss possible generalizations to other aeroelastic problems.

II. Rectangular Wing as a Toy Model

We consider a classical two-degree-of-freedom aeroelastic model of a thin unswept rectangular wing (Fig. 1), which was first studied by Goland [4]. We will follow the book of Ref. [3], where the equations of motion are derived in chapter 10.2 by using a simplified aerodynamic model. We will briefly rederive the equations of motion for the case of fully unsteady aerodynamics to analyze various simplifications, as well as the fully unsteady model.

The wing span is s and the chord is c. We will assume that the wing cross section is a thin plate so that the aerodynamic center is located at $c/4$ downstream from the leading edge, whereas the elastic axis is located at x_f from the leading edge. The two degrees of freedom correspond to bending and torsional modes, with EI and GJ being the bending and torsional stiffnesses, respectively (Fig. 1). Assuming simple bending and torsional shapes, the general wing motion has the form

*Head of Laboratory, Institute of Mechanics, 1, Leninskie Gory.
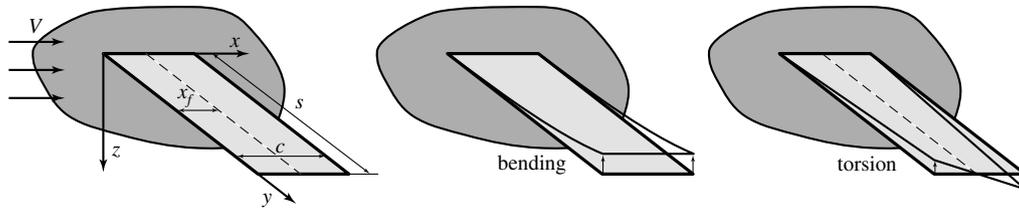
Fig. 1 Rectangular wing and its bending and torsional degrees of freedom.

$$z(x, y, t) = \left(\frac{y}{s}\right)^2 q_b(t) + \left(\frac{y}{s}\right)(x - x_f)q_t(t)$$

where q_b and q_t area the generalized coordinates corresponding to the bending and torsion. Applying Lagrange's equation as was done in Ref. [3] (Chap. 10.2.1), we find the equations of motion:

$$m\begin{pmatrix} \frac{sc}{5} & \frac{s}{4}\left(\frac{c^2}{2} - cx_f\right) \\ \frac{s}{4}\left(\frac{c^2}{2} - cx_f\right) & \frac{s}{3}\left(\frac{c^3}{3} - c^2 x_f + x_f^2 c\right) \end{pmatrix}\begin{pmatrix} \ddot{q}_b \\ \ddot{q}_t \end{pmatrix} + \begin{pmatrix} \frac{4EI}{s^3} & 0 \\ 0 & \frac{GJ}{s} \end{pmatrix}\begin{pmatrix} q_b \\ q_t \end{pmatrix}$$
$$= \begin{pmatrix} Q_b \\ Q_t \end{pmatrix} \tag{1}$$

where Q_b and Q_t are the generalized aerodynamic forces corresponding to the bending and torsional motions. To calculate Q_b and Q_t, consider the lift and moment produced by the flow. In this and the next section, we will restrict ourselves to the harmonic motion of the wing, which is sufficient for both divergence and flutter analyses.

To calculate the unsteady aerodynamic lift and moment, we will use a strip theory, assuming that aerodynamic forces produced by each cross section can be taken from a corresponding two-dimensional problem for a thin plate, where the lift-curve slope is 2π. Let the wing undergo harmonic motion with elastic axis deflection of $z = z_0 e^{i\omega t}$ and pitch of $\theta = \theta_0 e^{i\omega t}$. The two-dimensional aerodynamic forces are readily given by the Theodorsen theory, which is a linearized solution of the two-dimensional (2-D) problem for a thin oscillating plate in inviscid incompressible fluid flow (Ref. [5], Ref. [1] Chaps. 5–6, Ref. [2] Chap. 6.9, and Ref. [3] Chap. 9.3):

$$L = \left\{ \pi\rho b^2(-\omega^2 z_0 + i\omega V\theta_0 + \omega^2 ba\theta_0) \right.$$
$$\left. + 2\pi\rho VbC(k)\left(i\omega z_0 + V\theta_0 + i\omega b\left(\frac{1}{2} - a\right)\theta_0\right) \right\} e^{i\omega t}$$
$$M = \left\{ \pi\rho b^2\left(-\omega^2 baz_0 - i\omega Vb\left(\frac{1}{2} - a\right)\theta_0 + b^2\omega^2\left(\frac{1}{8} + a^2\right)\theta_0\right) \right.$$
$$\left. + 2\pi\rho Vb^2\left(\frac{1}{2} + a\right)C(k)\left(i\omega z_0 + V\theta_0 + i\omega b\left(\frac{1}{2} - a\right)\theta_0\right) \right\} e^{i\omega t} \tag{2}$$

Here, L and M are the 2-D aerodynamic lift force and moment with respect to the elastic axis, ρ and V are the flow density and velocity, $b = c/2$ is the semichord, $a = x_f/b - 1$ is a parameter of the elastic axis location with respect to the midchord, $k = \omega c/(2V) = \omega b/V$ is the reduced frequency, and $C(k)$ is the Theodorsen function defined as either

$$C_H(k) = \frac{H_1^{(2)}(k)}{H_1^{(2)}(k) + iH_0^{(2)}(k)} \tag{3}$$

or

$$C_K(k) = \frac{K_1(ik)}{K_0(ik) + K_1(ik)} \tag{4}$$

Note that functions defined by Eqs. (3) and (4) coincide for $\text{Re}\,k \geq 0$ so that the use of one of these formulas is identical for practical calculations. However, they have different branch cuts in the entire complex k plane, which is crucial for the correct analysis of eigenfrequency branches, as will be shown in the following. We also note that the oscillation frequency ω in Eq. (2) is not restricted to be real; that is, any sinusoidal, exponentially damped and exponentially growing motions are suitable. This fact is easily seen because $L(\omega)$ and $M(\omega)$ are analytical complex functions of ω, which means that, even if derived for real ω, those functions are analytically continued to the complex ω plane with branch cuts of $C(k)$ properly taken into account. As a historical note, a more general solution also accounting for deformable wings was independently obtained by Sedov [6] in 1936: one year after Theodorsen [5].

The expressions of Eq. (2) can be rewritten by using so-called oscillatory aerodynamic derivatives as follows:

$$L = \rho V^2 b\left\{(L_z + ikL_{\dot{z}})\frac{z_0}{b} + (L_\theta + ikL_{\dot{\theta}})\theta_0\right\} e^{i\omega t}$$
$$M = \rho V^2 b^2\left\{(M_z + ikM_{\dot{z}})\frac{z_0}{b} + (M_\theta + ikM_{\dot{\theta}})\theta_0\right\} e^{i\omega t} \tag{5}$$

where the oscillatory aerodynamic derivatives are (Ref. [3] Chap. 9.4)

$$L_z = 2\pi\left(-\frac{k^2}{2} - G(k)k\right), \quad L_{\dot{z}} = 2\pi F(k)$$
$$L_\theta = 2\pi\left(\frac{k^2 a}{2} + F(k) - G(k)k\left(\frac{1}{2} - a\right)\right),$$
$$L_{\dot{\theta}} = 2\pi\left(\frac{1}{2} + F(k)\left(\frac{1}{2} - a\right) + \frac{G(k)}{k}\right),$$
$$M_z = 2\pi\left(-\frac{k^2 a}{2} - G(k)k\left(\frac{1}{2} + a\right)\right), \quad M_{\dot{z}} = 2\pi\left(\frac{1}{2} + a\right)F(k)$$
$$M_\theta = 2\pi\left(\frac{k^2}{2}\left(\frac{1}{8} + a^2\right) + F(k)\left(\frac{1}{2} + a\right) - G(k)k\left(\frac{1}{2} + a\right)\left(\frac{1}{2} - a\right)\right),$$
$$M_{\dot{\theta}} = 2\pi\left(-\frac{1}{2}\left(\frac{1}{2} - a\right) + F(k)\left(\frac{1}{2} + a\right)\left(\frac{1}{2} - a\right) + \frac{G(k)}{k}\left(\frac{1}{2} + a\right)\right) \tag{6}$$

and $C(k) = F(k) + iG(k)$. Note that the expression for $M_{\dot{\theta}}$ in Ref. [3] (Chap. 9.4) has a misprint, and thus differs from the preceding formula.

To derive generalized aerodynamic forces Q_b and Q_t, consider the elementary work done by these forces over incremental deflections:

$$\delta W = \int_0^s L(y)\left(-\left(\frac{y}{s}\right)^2 \delta q_b\right) dy + \int_0^s M(y)\left(\frac{y}{s}\right)\delta q_t\, dy$$

In this expression, $L(y)$ and $M(y)$ are obtained from Eq. (5) by substitution of the bending and torsion span mode shapes: $z_0 = (y/s)^2 q_b$ and $\theta_0 = (y/s)q_t$. The minus sign in the work done by lift force is because the z axis is directed downward (Fig. 1) to be consistent with the notations of Ref. [3]. Performing calculations, we find

$$\delta W = -\rho V^2 b \delta q_b \left[(L_z + ikL_{\dot{z}}) \frac{s}{5} \frac{q_b}{b} + (L_\theta + ikL_{\dot{\theta}}) \frac{s}{4} q_t \right] e^{i\omega t}$$

$$+ \rho V^2 b^2 \delta q_t \left[(M_z + ikM_{\dot{z}}) \frac{s}{4} \frac{q_b}{b} + (M_\theta + ikM_{\dot{\theta}}) \frac{s}{3} q_t \right] e^{i\omega t}$$

Consequently,

$$\begin{pmatrix} Q_b \\ Q_t \end{pmatrix} = \begin{pmatrix} \dfrac{\partial(\delta W)}{\partial(\delta q_b)} \\ \dfrac{\partial(\delta W)}{\partial(\delta q_t)} \end{pmatrix} = \left(\rho V^2 \begin{pmatrix} \dfrac{s}{5}L_z & \dfrac{bs}{4}L_\theta \\ -\dfrac{bs}{4}M_z & -\dfrac{b^2 s}{3}M_\theta \end{pmatrix} \right.$$

$$\left. - i\omega\rho V \begin{pmatrix} \dfrac{sb}{5}L_{\dot{z}} & \dfrac{b^2 s}{4}L_{\dot{\theta}} \\ -\dfrac{b^2 s}{4}M_{\dot{z}} & -\dfrac{b^3 s}{3}M_{\dot{\theta}} \end{pmatrix} \right) \begin{pmatrix} q_b \\ q_t \end{pmatrix} \quad (7)$$

Substituting these expressions into Eq. (1), and recalling that $b = c/2$, we finally obtain aeroelastic equations of motion that yield the following eigenvalue problem:

$$\mathcal{F}(\omega) = \det(-\omega^2 M + i\omega D_a(k) + (K_a(k) + K)) = 0 \quad (8)$$

where

$$M = m \begin{pmatrix} \dfrac{sc}{5} & \dfrac{s}{4}\left(\dfrac{c^2}{2} - cx_f\right) \\ \dfrac{s}{4}\left(\dfrac{c^2}{2} - cx_f\right) & \dfrac{s}{3}\left(\dfrac{c^3}{3} - c^2 x_f + x_f^2 c\right) \end{pmatrix},$$

$$D_a(k) = \rho V \begin{pmatrix} \dfrac{sc}{10}L_{\dot{z}} & \dfrac{c^2 s}{16}L_{\dot{\theta}} \\ -\dfrac{c^2 s}{16}M_{\dot{z}} & -\dfrac{c^3 s}{24}M_{\dot{\theta}} \end{pmatrix},$$

$$K_a(k) = \rho V^2 \begin{pmatrix} \dfrac{s}{5}L_z & \dfrac{cs}{8}L_\theta \\ -\dfrac{cs}{8}M_z & -\dfrac{c^2 s}{12}M_\theta \end{pmatrix}, \quad K = \begin{pmatrix} \dfrac{4EI}{s^3} & 0 \\ 0 & \dfrac{GJ}{s} \end{pmatrix} \quad (9)$$

In this study, we neglect the structural damping for clarity because it does not affect the principal results in any way.

The eigenvalue problem [Eq. (8)] is not algebraic, as it might seem at first sight. Eigenfrequency ω is not only explicitly present in the equation but also implicitly present in aerodynamic matrices, which are functions of the reduced frequency of $k = \omega b/V$. Hence, we cannot a priori guarantee the existence of four (and only four) roots, which would be the case if aerodynamic matrices are independent from k. Moreover, in the following, we will show that the number of solutions changes when crossing the divergence speed.

The eigenvalue problem is solved numerically by an iterative method. At the first iteration, we assume $k = 0$, calculate the corresponding aerodynamic matrices ($M_{\dot{\theta}}$ and $L_{\dot{\theta}}$ are forced to be zero at the first iteration, as discussed in Ref. [3] (Chap. 9.4), and solve Eq. (8) with respect to ω, obtaining four roots: ω_n^0, $n = 1$–4. One of the roots is chosen and calculated by subsequent iterations. Assume that the jth iteration of the root ω^j is calculated. We recalculate $k^j = \omega^j b/V$, recalculate the aerodynamic matrices, and again solve Eq. (8) with respect to ω. Among the four roots, we choose the one closest to ω^j, which gives the next-iteration root ω^{j+1}. Iterations are repeated until the convergence is achieved with a given accuracy. For the case of slow convergence, which occurs near the divergence boundary, weighting of the $(j + 1)$th root is used with the relaxation coefficient $\varkappa = 0.1$: $\omega_{\text{final}}^{j+1} = (1 - \varkappa)\omega^{j+1} + \varkappa\omega^j$.

Calculations are started at sufficiently small V, where each solution is associated with a wing eigenmode in still air. Next, the velocity is gradually increased, with the initial guess of k taken from the converged solution from the previous step in velocity. In this way, we obtain a continuous branch of eigenfrequencies with the velocity V as a parameter.

We emphasize that the iterative procedure described converges to the exact solution of the eigenvalue problem [Eq. (8)] for any V: no matter if the eigenmode is damped, neutral, or growing. We will show in the following that the number of roots changes from four to five, where the additional solution is not a continuation of a natural frequency, so that the initial guess for this root should be different. Other well-known methods ("k," "p-k," and "g" methods) give the exact solution only for neutral oscillation, which corresponds to the critical divergence or flutter speed. These methods will be discussed in Sec. V.A.

In this study, we will not consider flutter but focus on transition to divergence. This transition, by definition, occurs through zero eigenfrequency. Putting $\omega = 0$ (and hence $k = 0$) and using $L_z(0) = 0$, $L_\theta(0) = 2\pi$, $M_z(0) = 0$, and $M_\theta(0) = 4\pi e$, where

$$e = ((1/2) + a)/2 = (x_f - (c/4))/c$$

is the distance from the aerodynamic center to the elastic axis rated to the chord, we immediately derive the divergence speed:

$$V_{\text{div}} = \sqrt{\frac{3GJ}{\rho c^2 s^2 e\pi}}$$

The next section is devoted to the divergence mechanism analysis.

III. Divergence Mechanism Through Simplified Aerodynamics

In the following calculations, we will use the parameters used in Ref. [3] (Chap. 10.8), which are given in Table 1, that correspond to the natural circular frequencies of the wing of $\omega_t = 8.92$ rad/s and $\omega_b = 17.83$ rad/s (torsional and bending, respectively) and the divergence speed of $V_{\text{div}} = 54.9$ m/s.

A. Quasi-Steady Aerodynamics

We start with the simplest aerodynamic formulation: quasi-steady aerodynamics. Taking the limit of $k \to 0$ and $C(k) \to 1$ in Eq. (6), we have

$$L_z = 0, \qquad L_{\dot{z}} = 2\pi, \qquad L_\theta = 2\pi, \qquad M_z = 0, \qquad M_{\dot{z}} = 4\pi e,$$

$$M_\theta = 4\pi e, \qquad e = \frac{1}{2}\left(\frac{1}{2} + a\right) \quad (10)$$

Terms $L_{\dot{\theta}}$ and $M_{\dot{\theta}}$ have singularities as $k \to 0$; but, as discussed in Ref. [3] (Chap. 9.4), they are present in Eq. (5) in combination with k and do not contribute to the quasi-steady lift and moment because $kL_{\dot{\theta}}(k) \to 0$ and $kM_{\dot{\theta}}(k) \to 0$ as $k \to 0$. Hence, the quasi-steady limit is reduced to

Table 1 Parameters used in calculations

Parameter	Value
Wing span s	7.5 m
Chord c	2 m
Elastic axis x_f	$0.48c$
Mass per unit area m	200 kg/m^2
Bending stiffness EI	2×10^7 N · m^2
Torsional stiffness GJ	2×10^5 N · m^2
Mass axis	$0.5c$
Air density ρ	1.225 kg/m^3

$$L = \rho V^2 b 2\pi \left\{ ik\frac{z_0}{b} + \theta_0 \right\} e^{i\omega t} = \frac{\rho V^2}{2} c \times 2\pi \left(\frac{\dot{z}}{V} + \theta \right)$$

$$M = \rho V^2 b^2 2\pi \left(\frac{1}{2} + a\right) \left\{ ik\frac{z_0}{b} + \theta_0 \right\} e^{i\omega t}$$

$$= \frac{\rho V^2}{2} c^2 \times 2\pi e \left(\frac{\dot{z}}{V} + \theta \right) = Lec \qquad (11)$$

which have a straightforward meaning: these are the steady aerodynamic lift and moment acting on a plate at an angle of attack θ corrected by an additional angle of attack $\dot{z}/V$ caused by a vertical motion of the wing.

Substitution into Eq. (8) yields the eigenvalue problem with the following aerodynamic matrices:

$$D_a = \rho V \begin{pmatrix} \dfrac{sc}{10}2\pi & 0 \\ -\dfrac{c^2 s}{8}e2\pi & 0 \end{pmatrix}, \qquad K_a = \rho V^2 \begin{pmatrix} 0 & \dfrac{sc}{8}2\pi \\ 0 & -\dfrac{c^2 s}{6}e2\pi \end{pmatrix}$$

The result of the calculations is shown in Fig. 2. At small V, the wing has four slightly damped eigenfrequencies close to natural frequencies: $\omega_{1,3} \approx \pm\omega_t$ (torsional mode) and $\omega_{2,4} \approx \pm\omega_b$ (bending mode). Two of them $\omega_{1,2}$ are located at the right-hand side of the complex ω plane; two more eigenfrequencies $\omega_{3,4}$ are located symmetrically with respect to the imaginary axis, and they correspond to exactly the same wing motions. When the velocity increases, torsional frequencies $\omega_{1,3}$ move toward each other, coalesce at the imaginary axis ω, and become pure imaginary. After the coalescence, one of the frequencies moves up and the corresponding mode is damped; whereas the other moves down, crosses at $V = V_{\text{div}}$ zero frequency, and the corresponding mode becomes unstable.

This mechanism is a classical transition to divergence. The divergence mode is generated by the interaction of the first (torsion) mode with its paired frequency due to negative aerodynamic stiffness.

B. Simplified Unsteady Aerodynamics with Real $M_{\dot{\theta}}$

Following the book of Ref. [3], we consider a more complicated aerodynamic model and include the unsteady term $M_{\dot{\theta}}$, which was shown to have the most important effect:

$$D_a = \rho V \begin{pmatrix} \dfrac{sc}{10}2\pi & 0 \\ -\dfrac{c^2 s}{8}e2\pi & -\dfrac{c^3 s}{24}M_{\dot{\theta}} \end{pmatrix}, \quad K_a = \rho V^2 \begin{pmatrix} 0 & \dfrac{sc}{8}2\pi \\ 0 & -\dfrac{c^2 s}{6}e2\pi \end{pmatrix} \quad (12)$$

As suggested in Ref. [3] (Chap. 9.6), the value $M_{\dot{\theta}} = -1.2$ is a good approximation for the practically important range of real k; that is why this value is taken as an example (the actual value is not important for the divergence mechanism discussed in the following).

The results of the calculations shown in Fig. 3 are similar to quasi-steady aerodynamics. The only change is that the coalescence occurs at a different velocity, which does not affect the divergence velocity.
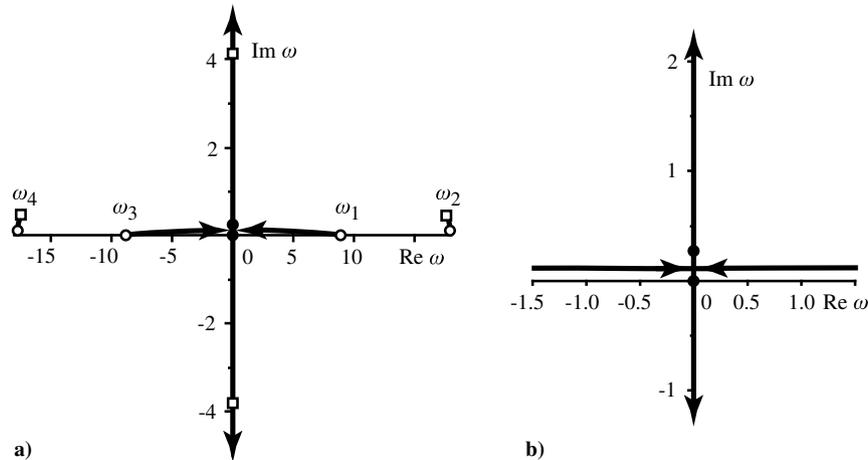
Fig. 2 Eigenfrequency loci in quasi-steady approximation when changing flow speed V from $V = 10$ m/s (open circles) to $V = V_{\text{div}} = 54.9$ m/s (filled circles) and further to $V = V_{\text{div}} + 5 = 59.9$ m/s (open squares): a) general view, and b) enlarged view around zero frequency.
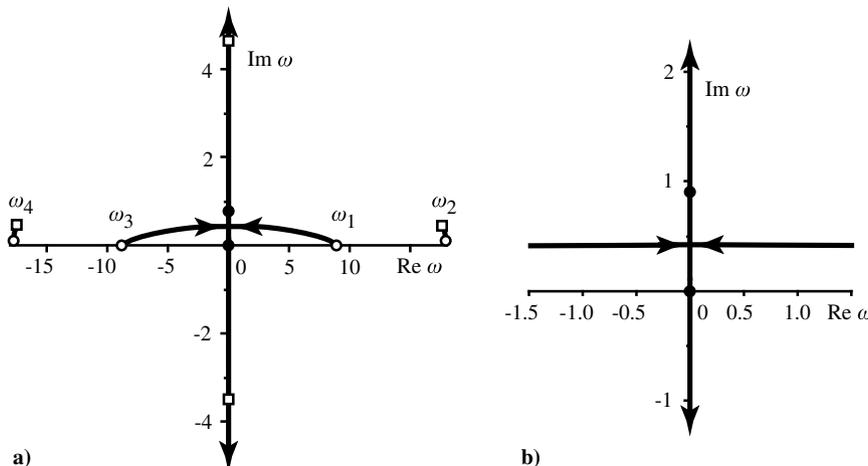
Fig. 3 Eigenfrequency loci calculated with simplified unsteady aerodynamics with real $M_{\dot{\theta}}$ when changing flow speed V from $V = 10$ m/s (open circles) to $V = V_{\text{div}} = 54.9$ m/s (filled circles) and further to $V = V_{\text{div}} + 5 = 59.9$ m/s (open squares): a) general view, and b) enlarged view around zero frequency.

However, the real value of $M_{\dot\theta}$ is not satisfactory because the modes are damped, the reduced frequencies k are complex, and the actual values of $M_{\dot\theta}$ should be complex.

C. Simplified Unsteady Aerodynamics with Complex $M_{\dot\theta}$

The easiest way to take the imaginary part of the reduced frequency into account is to consider the complex constant value of $M_{\dot\theta}$. The eigenvalue problem stays polynomial, but its coefficients become complex. Hence, the frequency coalescence (in general) does not occur at any V but changes to a hyperbola-type interaction. Figure 4 shows the results of the calculation for $M_{\dot\theta} = -1.2 + i$ and $M_{\dot\theta} = -1.2 + 2i$ (the value of the imaginary part does not qualitatively change the eigenfrequency loci), where, instead of coalescence, the eigenfrequencies approach and pass each other. The transition to divergence, of course, occurs at the same value $V_{\rm div}$ through zero frequency.

This type of mode interaction is common for binary (coupled-mode) flutter in many aeroelastic systems. However, the same interaction does not look satisfactory for the case of divergence. It was mentioned earlier in this paper that the eigenfrequencies with $\mathrm{Re}\,\omega > 0$ and $\mathrm{Re}\,\omega < 0$ must be exactly symmetrical with respect to the imaginary axis because they correspond to exactly the same wing motion. Indeed, for each frequency $\omega = \omega_r + i\omega_i$ and eigenvector

$$(X_b, X_t)^T = (X_{br} + iX_{bi}, X_{tr} + iX_{ti})^T$$

the complex motion is

$$\begin{pmatrix} q_b \\ q_t \end{pmatrix} = \begin{pmatrix} X_b \\ X_t \end{pmatrix} e^{i\omega t} = \begin{pmatrix} X_{br}\cos(\omega_r t) - X_{bi}\sin(\omega_r t) \\ X_{tr}\cos(\omega_r t) - X_{ti}\sin(\omega_r t) \end{pmatrix} e^{-\omega_i t}$$
$$+ i\begin{pmatrix} X_{bi}\cos(\omega_r t) + X_{br}\sin(\omega_r t) \\ X_{ti}\cos(\omega_r t) - X_{tr}\sin(\omega_r t) \end{pmatrix} e^{-\omega_i t}$$

Keeping in mind that only the real and imaginary parts of this expression separately have physical meaning, we can see that eigenfrequency $\omega = -\omega_r + i\omega_i$ and eigenvector

$$(X_b, X_t)^T = (X_{br} - iX_{bi}, X_{tr} - iX_{ti})^T$$

correspond to the same real and imaginary parts, i.e., the same physical motion. Hence, the symmetry of the eigenfrequencies with respect to the imaginary axis is a fundamental property of any aeroelastic system. However, this fundamental symmetry is absent in Fig. 4, and it will obviously be absent for any constant complex value of $M_{\dot\theta}$.

A naive solution would consist of considering different constant $M_{\dot\theta}$ for $\mathrm{Re}\,\omega > 0$ and $\mathrm{Re}\,\omega < 0$ changing in the sign of $\mathrm{Im}\,M_{\dot\theta}$. This yields
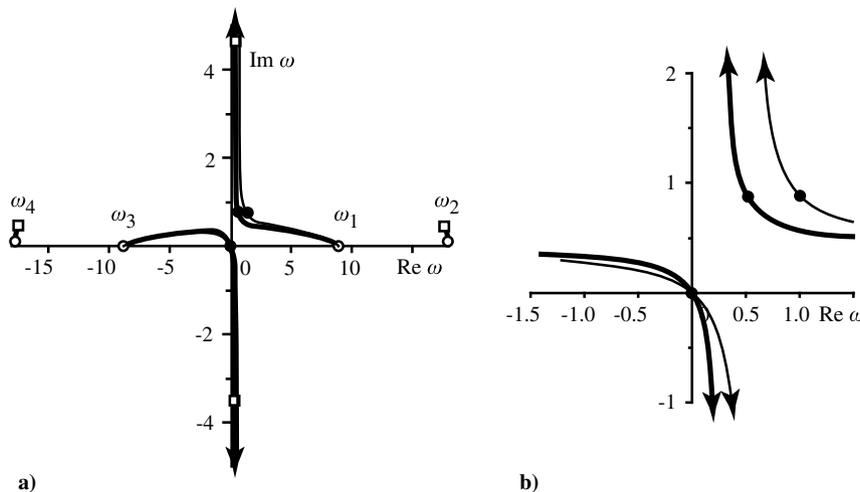
symmetrical loci of ω_1 and ω_3, but they both stay damped and none of them transforms to the divergence mode. On the other hand, the divergence mode does exist because $\omega = 0$ and $V = V_{\rm div}$ satisfies not only the eigenvalue problem with simplified matrices [Eq. (12)] but even with exact matrices [Eq. (9)]. As this divergence eigenfrequency is not a continuation of the natural frequency branches, it is not clear where it comes from.

To resolve this problem, we now switch to full unsteady aerodynamics defined by Eq. (9), and we reanalyze the divergence mechanism, which is a matter in the next section of the paper.

IV. Divergence Mechanism Through the Full Unsteady Aerodynamics

A. Divergence Modeling Using the Full Theodorsen Theory

When using full Theodorsen aerodynamics [Eq. (9)], the behavior of the ω_1 and ω_3 curves becomes symmetrical, but they both become highly damped (Fig. 5) because $M_{\dot\theta}$, which plays a major role, becomes essentially complex and $\mathrm{Im}\,M_{\dot\theta}(k_1)$ rapidly grows when $\mathrm{Re}\,\omega_1$ decreases, as shown in Fig. 6 [note that $M_{\dot\theta}(k_3) = \bar{M}_{\dot\theta}(k_1)$]. However, if we take the divergence mode (i.e. $V = V_{\rm div}$ and $\omega = 0$) as an initial guess and conduct calculations at $V > V_{\rm div}$, the numerical processes converges and give the fifth eigenfrequency branch (Fig. 5).

To analyze where the divergence mode transforms to at low flow speeds, we started decreasing the speed. However, surprisingly, the numerical procedure diverges for any velocity lower than $V_{\rm div}$, and so
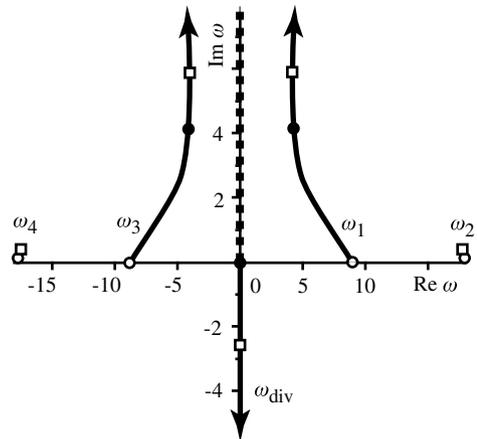
Fig. 5 Eigenfrequency loci calculated through full unsteady aerodynamics when changing flow speed V from $V = 10$ m/s (open circles) to $V = V_{\rm div} = 54.9$ m/s (filled circles) and further to $V = V_{\rm div} + 5 = 59.9$ m/s (open boxes). Dashed curve shows the continuous spectrum.

a)   b)

Fig. 4 Eigenfrequency loci calculated with simplified unsteady aerodynamics with complex $M_{\dot\theta}$ when changing flow speed V from $V = 10$ m/s (open circles) to $V = V_{\rm div} = 54.9$ m/s (filled circles) and further to $V = V_{\rm div} + 5 = 59.9$ m/s (open squares): a) general view, and b) enlarged view around zero frequency. $M_{\dot\theta} = -1.2 + i$ (bold lines), and $M_{\dot\theta} = -1.2 + 2i$ (thin lines).
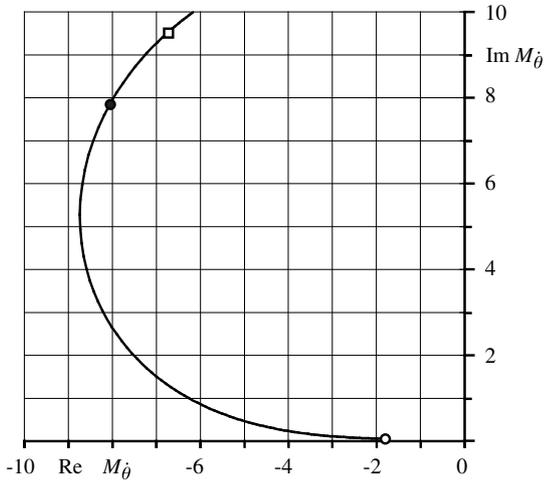
Fig. 6 $M_{\dot{\theta}}(k_1)$ **change when changing flow speed** V **from** $V = 10$ **m/s (open circle) to** $V = V_{\text{div}} = 54.9$ **m/s (filled circle) and further to** $V = V_{\text{div}} + 5 = 59.9$ **m/s (square).**

it could be thought that this mode comes from "nowhere," i.e., has no continuation from supercritical to subcritical speeds. To demonstrate

$$L_z = -2\pi k \mathrm{Re}k \, \ell_n \left| \frac{k}{2} \right|, \qquad L_{\dot{z}} = 2\pi \left(1 - \mathrm{Im}k \, \ell_n \left| \frac{k}{2} \right| \right),$$

$$L_\theta = 2\pi \left(1 - \mathrm{Im}k \left(\gamma + \ell_n \left| \frac{k}{2} \right| \right) - \mathrm{Re}k \mathrm{Arg}(ik) - k\mathrm{Re}k \, \ell_n \left| \frac{k}{2} \right| \left(\frac{1}{2} - a \right) \right),$$

$$L_{\dot{\theta}} = 2\pi \left(\frac{1}{2} + \left(1 - \mathrm{Im}k \, \ell_n \left| \frac{k}{2} \right| \right) \left(\frac{1}{2} - a \right) + \frac{\mathrm{Re}k}{k} \left(\gamma + \ell_n \left| \frac{k}{2} \right| \right) - \frac{\mathrm{Im}k}{k} \mathrm{Arg}(ik) \right),$$

$$M_z = -2\pi k \mathrm{Re}k \, \ell_n \left| \frac{k}{2} \right| \left(\frac{1}{2} + a \right), \qquad M_{\dot{z}} = 2\pi \left(\frac{1}{2} + a \right) \left(1 - \mathrm{Im}k \, \ell_n \left| \frac{k}{2} \right| \right),$$

$$M_\theta = 2\pi \left(\left(1 - \mathrm{Im}k \left(\gamma + \ell_n \left| \frac{k}{2} \right| \right) - \mathrm{Re}k \mathrm{Arg}(ik) \right) \left(\frac{1}{2} + a \right) - k\mathrm{Re}k \, \ell_n \left| \frac{k}{2} \right| \left(\frac{1}{2} + a \right) \left(\frac{1}{2} - a \right) \right),$$

$$M_{\dot{\theta}} = 2\pi \left(-\frac{1}{2} \left(\frac{1}{2} - a \right) + \left(1 - \mathrm{Im}k \, \ell_n \left| \frac{k}{2} \right| \right) \left(\frac{1}{2} + a \right) \left(\frac{1}{2} - a \right) + \left(\frac{\mathrm{Re}k}{k} \left(\gamma + \ell_n \left| \frac{k}{2} \right| \right) - \frac{\mathrm{Im}k}{k} \mathrm{Arg}(ik) \right) \left(\frac{1}{2} + a \right) \right)$$

that the absence of the divergence mode for $V < V_{\text{div}}$ is not a numerical issue but a real phenomenon, we give a rigorous proof in the next section.

B. Proof of the Nonexistence of the Divergence Mode at Subcritical Flow Velocity

Let us have the solution $\omega = k = 0$ at $V = V_{\text{div}}$. We take a small velocity deviation $V = V_{\text{div}} + V'$ and find a solution of Eq. (8) that tends to zero as $V' \to 0$; i.e., we find the divergence mode frequency in the vicinity of the divergence boundary.

Neglecting the ω^2 term as infinitesimal and combining aerodynamic damping and stiffness matrices, we have the eigenvalue problem [Eq. (8)] in the following form:

$$\det \left(\rho(V_{\text{div}} + V')^2 \begin{pmatrix} \frac{s}{5}(L_z + ikL_{\dot{z}}) & \frac{cs}{8}(L_\theta + ikL_{\dot{\theta}}) \\ -\frac{cs}{8}(M_z + ikM_{\dot{z}}) & -\frac{c^2s}{12}(M_\theta + ikM_{\dot{\theta}}) \end{pmatrix} \right.$$
$$\left. + \begin{pmatrix} \frac{4EI}{s^3} & 0 \\ 0 & \frac{GJ}{s} \end{pmatrix} \right) = 0 \qquad (13)$$

To obtain aerodynamic derivatives for small k, consider the asymptotic expansion of modified Bessel functions of the second kind at small z (Ref. [7] Chaps. 9.6.9 and 9.6.54):

$$K_0(z) \sim -\ell_n \left(\frac{z}{2} \right) - \gamma, \qquad K_\alpha(z) \sim \frac{\Gamma(\alpha)}{2} \left(\frac{2}{z} \right)^\alpha, \qquad \alpha > 0$$

where γ is the Euler–Mascheroni constant; hence, for small $|k|$, we have the following form of the Theodorsen function [Eq. (4)]:

$$C(k) \sim \frac{1/(ik)}{1/(ik) - \ell_n(ik/2) - \gamma} \sim 1 + ik \left(\gamma + \ell_n \left| \frac{k}{2} \right| \right) - k\mathrm{Arg}(ik),$$

$$F(k) = \mathrm{Re}C(k) \sim 1 - \mathrm{Im}k \left(\gamma + \ell_n \left| \frac{k}{2} \right| \right) - \mathrm{Re}k\mathrm{Arg}(ik),$$

$$G(k) = \mathrm{Im}C(k) \sim \mathrm{Re}k \left(\gamma + \ell_n \left| \frac{k}{2} \right| \right) - \mathrm{Im}k\mathrm{Arg}(ik)$$

where $\mathrm{Arg}(ik)$ is the principal argument. Then, from Eq. (6), we obtain aerodynamic derivatives at a small reduced frequency by neglecting terms of the order of k^2 and smaller in the z and θ derivatives, as well as by neglecting terms of the order of k and smaller in the $\dot{z}$ and $\dot{\theta}$ derivatives:

Substituting into Eq. (13); retaining terms of the order of V', k, and $k \, \ell_n \, k$; and neglecting higher terms, after some algebra; we have

$$k \left(a \frac{1 - 2a}{1 + 2a} + \gamma + \ell_n \left| \frac{k}{2} \right| + i\mathrm{Arg}(ik) - \rho V_{\text{div}}^2 \frac{3}{2} \frac{s^4}{4EI} \right) = 2i \frac{V'}{V_{\text{div}}}$$

Taking separately the real and imaginary parts of this equation, we obtain the system

$$\mathrm{Re}k \left(a \frac{1 - 2a}{1 + 2a} + \gamma + \ell_n \left| \frac{k}{2} \right| - \rho V_{\text{div}}^2 \frac{3}{2} \frac{s^4}{4EI} \right) - \mathrm{Im}k\mathrm{Arg}(ik) = 0,$$

$$\mathrm{Im}k \left(a \frac{1 - 2a}{1 + 2a} + \gamma + \ell_n \left| \frac{k}{2} \right| - \rho V_{\text{div}}^2 \frac{3}{2} \frac{s^4}{4EI} \right) + \mathrm{Re}k\mathrm{Arg}(ik) = 2 \frac{V'}{V_{\text{div}}} \qquad (14)$$

Now, consider three options:

1) The first option is $\mathrm{Im}k = 0$. With this option, we cannot satisfy both equations of Eq. (14); i.e., no real solution exists.

2) The second option is $\mathrm{Re}k = 0$. From the first equation of Eq. (14), we immediately obtain $\mathrm{Arg}(ik) = 0$, i.e., $k = -i\varkappa$, $\varkappa \in \mathbb{R}$, and $\varkappa > 0$. The leading term of the second equation of Eq. (14) is

$$-\varkappa \ell n \left| \frac{\varkappa}{2} \right| = 2 \frac{V'}{V_{\text{div}}}$$

This equation has a positive real solution $\varkappa(V')$ for $V' > 0$. This solution corresponds to the divergence eigenmode, and it exists only for $V' \geq 0$. Indeed, for $V' < 0$, we have $\varkappa(V') < 0$ and $\text{Arg}(ik) = \pi$, which does not satisfy the first equation of Eq. (14).

3) The third option is $\text{Re}k \neq 0$ and $\text{Im}k \neq 0$. It is sufficient to consider only $\text{Re}k > 0$ because the problem [Eq. (14)] is symmetrical with respect to the imaginary axis k. Retaining only the leading logarithmic term in the first terms of Eq. (14), they can be rewritten as

$$\frac{|k|^2}{\text{Im}k} \ell n \left| \frac{k}{2} \right| = 2 \frac{V'}{V_{\text{div}}}, \qquad \frac{|k|^2}{\text{Re}k} \text{Arg}(ik) = 2 \frac{V'}{V_{\text{div}}}$$

Dividing the second equation by the first and introducing $\alpha = \text{Arg}k$, we have

$$\tan \alpha \left(\frac{\pi}{2} + \alpha \right) \left(\ell n \left| \frac{k}{2} \right| \right)^{-1} = 1$$

Because $\ell n |k/2| < 0$ for small $|k|$, we conclude that $-\pi/2 < \alpha < 0$. However, the function $\tan \alpha(\pi/2 + \alpha)$ is bounded in this interval, whereas $\ell n |k/2| \to -\infty$ as $k \to 0$. Hence, no solution of this kind exists for small k.

We have proved that, at a flow speed slightly exceeding V_{div}, a growing divergence mode exists for which the frequency tends to zero as $V \to V_{\text{div}} + 0$; but, no mode exists for $V < V_{\text{div}}$. In other words, the divergence mode is not a continuation of a natural mode of the wing but is an additional eigenmode that exists only for $V \geq V_{\text{div}}$. This phenomenon is due to the logarithmic singularity of the Theodorsen function at $k = 0$, and it does not manifest itself if simplified aerodynamics is used.

The fact that, for the same aeroelastic system, there are four eigenmodes at $V < V_{\text{div}}$ and five eigenmodes at $V \geq V_{\text{div}}$ looks unusual, especially when considering that the number of eigenmodes in "regular" systems should be equal to the number of initial conditions that must be imposed in the initial-value problem. To resolve this phenomenon, we now consider the solution of the initial-value problem.

C. Divergence in the Framework of Initial-Value Problem

To formulate the initial-value problem, consider equations of motion [Eq. (1)] yielding the eigenvalue problem [Eq. (8)]. The generalized aerodynamic forces Q_b and Q_t are expressed through aerodynamic damping and stiffness matrices only for harmonic motion, where the Theodorsen aerodynamics is the linearized solution of the two-dimensional aerodynamic problem. For the case of the general time-domain motion, Q_b and Q_t are functions of t that can be written in the form of convolution integrals for which the kernels are expressed through the Wagner function (Ref. [1] Chaps. 5–7, Ref. [2] Chap. 6.7). Their exact form is now not important; the only principal point is that the Laplace transformation of $Q_{b,t}$ yields Theodorsen aerodynamics because Wagner and Theodorsen functions are related through the Laplace transformation (Ref. [1] Chaps. 5–7).

With the equations of motion, we specify the following initial conditions:

$$q_b(0) = q_b^0, \qquad \dot{q}_b(0) = q_b^1, \qquad q_t(0) = q_t^0, \qquad \dot{q}_t(0) = q_t^1,$$
$$q_{b,t}(t) = \dot{q}_{b,t}(t) = 0, \qquad t < 0$$

where q_b^n and q_t^n are given constants. Note that, as aerodynamic loads are calculated as convolution integrals of the wing displacement and velocity, not only initial conditions at $t = 0$ but the total preceding motion history for $t < 0$ must be specified. Physically, this feature reflects the effect of the wake behind the wing: the wake is convected downstream but "remembers" the wing motion in the past. That is why the aerodynamic loading at a given $t = t_0$ depends not only on instant deflection and the velocity of the wing but also on the wing

motions at preceding moments of time $t < t_0$. Here, to be specific, without loss of generality, we assume that the wing is at rest for $t < 0$.

To solve the integrodifferential system of Eq. (1) with the given initial conditions, we perform the Laplace transformation defined as

$$\xi_{b,t}(\omega) = \xi(\omega)\{q_{b,t}\} = \int_0^{+\infty} q_{b,t}(t) e^{-i\omega t} \, \mathrm{d}t$$

In contrast to the classical definition with the parameter s, we use the parameter $\omega = -is$ to more evidently connect the solution of the initial-value problem with the eigenvalue problem. Integrating by parts, we find

$$\xi(\omega)\{\dot{q}\} = -q^0 + i\omega\xi(\omega)\{q\}, \quad \xi(\omega)\{\ddot{q}\} = -q^1 - i\omega q^0 - \omega^2\xi(\omega)\{q\}$$

Then, the transformed system of equations [Eq. (1)] is as follows:

$$(-\omega^2 \mathbf{M} + i\omega \mathbf{D}_a(k) + (\mathbf{K}_a(k) + \mathbf{K})) \begin{pmatrix} \xi_b \\ \xi_t \end{pmatrix} = \begin{pmatrix} P_b \\ P_t \end{pmatrix} \qquad (15)$$

where $P_{b,t}$ are functions of the initial conditions $q_{b,t}^n$ and ω. We used here the fact that the Laplace transformation of the time-domain generalized aerodynamic forces yields the frequency-domain Theodorsen aerodynamics. We then solve this linear algebraic system by using Cramer's rule to obtain the Laplace transformation of the solution:

$$\xi_b = \frac{C_b(q_{b,t}^n, \omega)}{\mathcal{F}(\omega)}, \qquad \xi_t = \frac{C_t(q_{b,t}^n, \omega)}{\mathcal{F}(\omega)} \qquad (16)$$

Here, $\mathcal{F}(\omega)$ is the determinant [Eq. (8)] of the system of equations [Eq. (15)], and $C_{b,t}$ are determinants of the same matrix where either the first or second column is substituted by the right-hand side of the system.

Now, let us apply the inverse Laplace transformation to Eq. (16) by using Mellin's inverse formula [8]:

$$q_{b,t}(t) = \frac{1}{2\pi} \int_{-\infty - i\zeta}^{+\infty - i\zeta} \xi_{b,t}(\omega) e^{i\omega t} \, \mathrm{d}\omega \qquad (17)$$

where the integration path Γ is a horizontal line at the complex ω plane located below all singularities of $\xi_{b,t}(\omega)$ (Fig. 7). Again, the classical Mellin's formula deals with the parameter s of Laplace transformation, and the integration path is a vertical line located to the right of all singularities. Here, we use the parameter $\omega = -is$ so that the complex ω plane is the s plane rotated by $-\pi/2$.

Next, we move up the integration path Γ. The integral [Eq. (17)] is not changed due to the Cauchy theorem. This theorem, however, deals with integrals along finite-length paths, and so it should be used with care when we move the infinite-length line. However, it is easy to prove that the value of the integral still does not change (we do not give the proof here to avoid technical details).

The motion of the integration path goes well while the integrand does not have singularities. There are two types of singularities. The first type is zeros ω_n of the denominator [Eq. (16)], where the
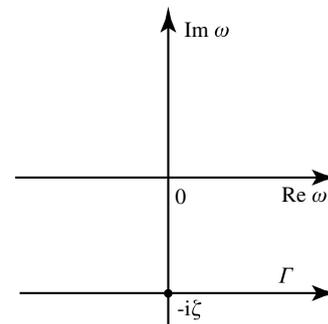
Fig. 7 Integration path Γ in Eq. (17).

integrand has poles. When passing through poles, the integral along the closed path surrounding the pole is separated (Fig. 8), which is calculated according to the residue theorem:

$$q_{b,t}(t) = \frac{1}{2\pi} \int_{\Gamma_1} \xi_{b,t}(\omega) e^{i\omega t} \, d\omega$$

$$= \frac{1}{2\pi} \int_{\Gamma_2} \xi_{b,t}(\omega) e^{i\omega t} \, d\omega + i \frac{C_{b,t}(q_{b,t}^n, \omega_n)}{d\mathcal{F}(\omega_n)/d\omega} e^{i\omega_n t}$$

Thus, each crossing of the eigenfrequency yields the separation of the corresponding eigenmode term from the integral.

The second type of singularity is the branch point of the Theodorsen function at $\omega = k = 0$. To deal with this singularity, we must properly define the branch cut. The two definitions of the Theodorsen function [Eqs. (3) and (4)] coincide at $\mathrm{Re}\,k \geq 0$ but differ in the branch cut. The first definition [Eq. (3)] has a branch cut along a real negative ray ($\mathrm{Im}\,k = 0$ and $\mathrm{Re}\,k \leq 0$), whereas the second has a branch cut along an imaginary positive ray ($\mathrm{Re}\,k = 0$ and $\mathrm{Im}\,k \geq 0$). The first definition lacks the fundamental symmetry of the aerodynamic forces because $k_1 = k_r + ik_i$ and $k_2 = -k_r + ik_i$ must correspond to exactly the same motion of the wing, but $C_H(k_1) \neq \bar{C}_H(k_2)$. The second definition [Eq. (4)] possesses this symmetry such that $C_K(k)$ is the only correct analytical continuation of the Theodorsen function from the right half-plane to the entire complex k plane. Having now the branch cut along an imaginary positive ray, we deform the integration path to embrace both sides of the branch cut (Fig. 9). The rest of the integration path moves to $\mathrm{Im}\,k \to +\infty$, where the integrand is an exponentially damped function with an arbitrarily large damping rate; and the value of this portion of the integral is zero. The integral over the branch cut cannot be improved, and so the final solution of the initial-value problem is

$$q_{b,t}(t) = \frac{1}{2\pi} \int_0^{+i\infty} [\xi]_{b,t}(\omega) e^{i\omega t} \, d\omega + \sum_{n=1}^{p} i \frac{C_{b,t}(q_{b,t}^n, \omega_n)}{d\mathcal{F}(\omega_n)/d\omega} e^{i\omega_n t} \quad (18)$$

where $[\xi]$ is the jump of ξ on the branch cut, and p is the number of eigenfrequencies.

We conclude that the general solution of the initial-value problem is the linear combination of two terms: eigenmodes that form the discrete spectrum of the problem, and the integral over pure imaginary damped frequencies that form a continuous spectrum. A similar result was obtained in Refs. [9,10] for a more general problem formulation. Note

that the proof of the continuous spectrum's existence is similar to the hydrodynamic stability theory problems, such as the solution to the initial-value problem for plane Coutte flow [11] that does not have a discrete spectrum at all but has a continuous spectrum that forms the solution.

The physical nature of the continuous spectrum originates from the wake behind the wing. As discussed earlier in this paper, the wake "memory" of the wing motion in the past results in aerodynamic loads depending not only on the instant wing position and velocity but also on all the preceding motion history. The continuous spectrum expresses the wake memory effect.

Recall that, mathematically, the presence of the continuous spectrum is the result of the branch cut of the Theodorsen function. It is now clear that the divergence eigenmode that exists only at $V \geq V_{\mathrm{div}}$ (Fig. 5) does not come from nowhere but separates from the continuous spectrum at $V = V_{\mathrm{div}}$. If simplified aerodynamics is used (such as in Secs. III.A and III.B), then the corresponding aerodynamic derivatives are holomorphic functions at the entire complex k plane so that $[\xi] = 0$, and no continuous spectrum is present. This reflects the fact that, physically, quasi-steady aerodynamics ignores the wake behind the wing and, consequently, the wake influence on the aerodynamic loads. In this formulation, the divergence mode is the continuation of the natural mode branch, according to the classical divergence mechanism described in textbooks [1–3].

V.   Comparison with Other Studies

A.   "Practical" Methods of Flutter Analysis

The results of this study deal with an "exact" eigenvalue problem, for which the numerical solution converges to the exact solution of the eigenvalue problem. Let us now consider several methods used in industrial flutter problems. First, the well-known k method imposes structural damping to make the aeroelastic system neutrally stable, and the instability is detected by positive imposed damping. In this method, because only neutral oscillations are considered, the reduced frequency k is always real so that no continuous spectrum can be detected, and the divergence is obtained due to eigenmode interaction, which is similar to quasi-steady aerodynamics. However, it is well known that the k method gives the correct result only for a stability boundary, where the oscillations are truly harmonic, but it has no physical meaning before and beyond the onset of instability. As an example, unphysical "folding" (appearance of multivalued frequency and damping functions of velocity) of $V - f$ and $V - g$
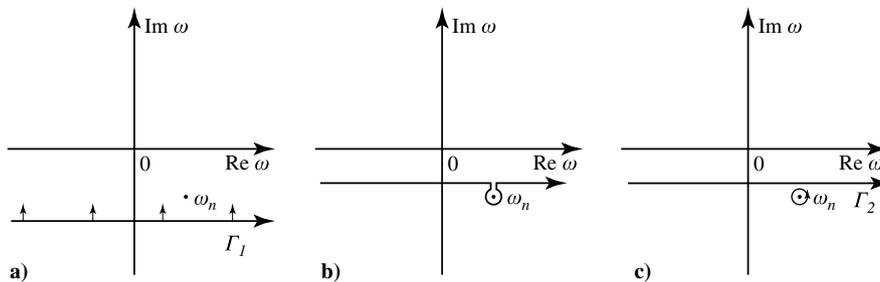
Fig. 8   Passing of integration path Γ through a pole ω_n: a) original path (horizontal line), b) deformed path, and c) final path split into a horizontal line above the pole and a closed path surrounding the pole.
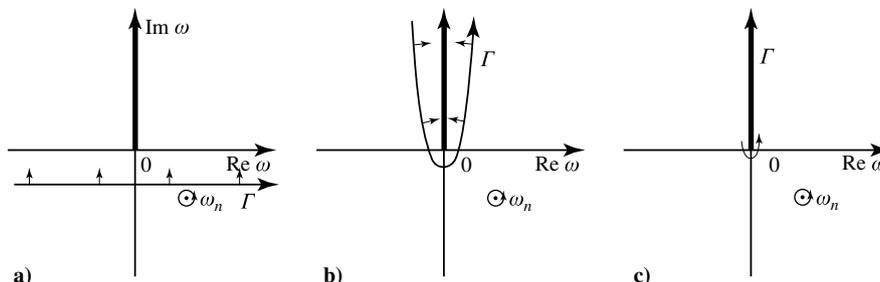
Fig. 9   Deformation of integration path around branch cut (shown by bold line): a) original path, b) path deformed to envelope branch cut, and c) final path consisting of two sides of branch cut.

curves is a typical situation (Ref. [3] Chap. 10.9.1) that occurred, for example, in Fig. 1 of Ref. [12] and in Fig. 4 of Ref. [13]. Also, the mode going to divergence or flutter can be predicted incorrectly [12]. The absence of the continuous spectrum is also an unphysical feature of this method.

The other two methods (p-k method [12] and g method [14,15]) assume that generalized aerodynamic forces can be calculated only for pure sinusoidal motion: $\omega \in \mathbb{R}$. Although k and "original" p-k methods use aerodynamic forces only for neutral oscillations (thus being correct only at stability boundary), the modified p-k method [16] and g method take the modal damping into account in aerodynamic force calculation, but through an approximate Taylor expansion. In the latter two methods, in addition to structural modes, the so-called "aerodynamic lag modes" appear [14,17,18]. The nature of these additional modes consists of the following. When the initial-value problem is solved, the Wagner function or Theodorsen function (whatever is used for calculating aerodynamic forces) is approximated by elementary functions, such as exponents (so-called Jones approximation) [10,17]. When such an approximation is used, the branch cut disappears; instead, several poles lying on a positive imaginary axis appear, as discussed in Ref. [10]. In other words, the continuous spectrum breaks up into a finite number of aerodynamic lag discrete modes. When analyzing the problem with this approximation, it was noted [14,17] that divergence occurs not when the structural eigenfrequency falls to zero but when the aerodynamic lag mode loses stability; whereas all structural modes stay damped. It is seen from our results and the study in Ref. [10] that these aerodynamic lag modes are artificial and appear only because of the approximation of aerodynamic transfer functions; whereas with exact Theodorsen aerodynamics, there is "an infinite number of aerodynamic lag modes" in terms of Refs. [10,17] or, in our terms, they form a continuous spectrum.

However, in contrast to the previously known structure of eigenmodes, our results show that, when the divergence speed is exceeded, the divergence mode is not a continuation of the aerodynamic lag mode but a truly new eigenmode that separates from the continuous spectrum. Note that the divergence mode existing apart from structural modes was also briefly mentioned in Ref. [9].

One more note should be made regarding the g method [14,15]. This method of modal damping inclusion into the aerodynamic force matrix is based on a Taylor expansion of $Q(\omega)$ at small $g = -\mathrm{Im}\,\omega$. Such an expansion is valid at points where the aerodynamic force is analytic. But, at $\omega = 0$, it has a logarithmic-type branch point (Sec. IV.B) because of the similar singularity of the Theodorsen function. Hence, the Taylor expansion at $\omega = k = 0$ is invalid, and so the V-g and V-f plots obtained by this method are inaccurate in the vicinity of the divergence speed, although the speed itself is predicted correctly.

B. Aeroelastic Analyses Through the Full Theodorsen Theory

The existence of the continuous spectrum in the aeroelastic system modeled through the exact Theodorsen theory was previously shown in Ref. [9]. Moreover, it was proved [10] that not only the incompressible 2-D Theodorsen solution but any compressible subsonic three-dimensional (3-D) solution for the aerodynamic loads has a branch cut; consequently, the corresponding aeroelastic system has a continuous spectrum along a positive imaginary ray. However, no connection between the continuous spectrum and the divergence mechanism was established in those studies.

Although there are a lot of papers using various approximations and numerical techniques, an aeroelastic analysis through the exact Theodorsen theory was conducted in a limited number of studies [9,19–21], where the work [20] was one in which the transition to divergence was observed. The figures of (Ref. [20] Figs. 3, 4, and 11) and the corresponding discussion clearly indicate that the loci of the structural eigenfrequencies do not coalesce and do not yield the divergence eigenmode. The latter, exactly as in the present study, does not exist for $V < V_{\mathrm{div}}$ and appears only at $V \geq V_{\mathrm{div}}$, starting from a zero frequency. However, it seems that the relation between the existence of the divergence mode only at $V \geq V_{\mathrm{div}}$ and the continuous spectrum was not established in that study.

C. Numerical Studies

Let us now consider representation of the continuous spectrum obtained through various numerical methods. First, as already noted earlier in this paper, the Jones approximation of the Wagner function yields the corresponding approximation of the Theodorsen function as a rational function [9]. In addition to structural roots, the appearance of two aerodynamic lag roots was observed [14,17,18] such that the divergence was originated from those aerodynamic lag modes but not the structural modes. It is important to note that, in those studies, such additional modes were not always present but had their respective "activation velocities," i.e., velocities at which they appeared. The concept of the activation velocity of a mode does not have an equivalent in the exact theory because the continuous spectrum consisting of all monotonically damped frequencies exists at any positive flow speed.

A more general approximation of the Theodorsen function is given by the Padé approximation. It was shown [22] that this yields the breakup of the continuous spectrum into a finite number of additional aerodynamic modes. The author is not aware of any attempts of a divergence analysis through the Padé approximation; however, it is expected that, similar to Refs. [14,17,18], these modes will lose stability instead of the structural modes.

A totally different approach was used in the work of Ref. [23]. The time-domain vortex-lattice method was used, and the results of the calculations were transformed to the frequency domain. First, it was observed that, besides the structural frequencies, there exist hundreds (equal to the number of vortex elements along the wake) of frequencies that represent the unsteady wake behind the wing. Although not all those frequencies correspond to the monotonically damped motion, the oscillating part of the motion was diminished when the numerical resolution was increased (e.g., see Fig. 5 of Ref. [23]). At that, the number of additional frequencies increased when the numerical resolution (i.e., the number of vortex elements along the wing surface and the wake) was increased. The principal conclusion of the numerical part of that study was the divergence originating from aerodynamic but not structural mode (see Fig. 24a of Ref. [23]). From the point of view of the exact theory, it is clear that the vortex-lattice method represents the continuous spectrum as a large but finite number of discrete modes in exactly the same manner that the time-domain motion of the wake calculated through the vortex-lattice method represents its exact motion.

D. Experimental Study

Finally, the most impressive evidence of the divergence not originating from a structural mode was given by the experimental part of Ref. [23]. In the course of the wind-tunnel experiment on a quasi-2-D wing, the frequency and damping of each structural mode were continuously and carefully measured and tracked in air-on conditions. It was shown that, when increasing the flow speed, the frequencies and damping did not approach zero when the flow speed approached the divergence speed (see discussion on pp. 79–80 and 109–118 of Ref. [23]). On the contrary, the divergence appeared suddenly, without any precursor in the structural modes. This indicated the agreement between the experiment and the numerical analysis [23], and it is in agreement with the general theory of the present paper. A similar experimental result of divergence not originating from the structural mode interaction was obtained in Ref. [24].[†]

VI. Conclusions

We have shown that, when modeling unsteady aerodynamics using the full Theodorsen theory, transition to divergence occurs not because of the mode coalescence and passing through zero frequency but through the appearance of an additional divergence mode that exists at postdivergence speeds but is absent at subcritical speeds. This mode separates at $V = V_{\mathrm{div}}$ from the continuous spectrum (Fig. 5) that corresponds to purely imaginary damped frequencies (including zero frequency), and therefore cannot yield the instability but produces the growing divergence mode. The existence of a

---

[†]According to a private communication with Professor Earl Dowell, Duke University, Durham, NC, 29 August 2019.

continuous spectrum is seen in the general solution of the initial-value problem and results from the branch cut of the Theodorsen function. Physically, it reflects the influence of the wake behind the wing on the aerodynamic loads of the aeroelastic system.

The appearance of a new, fifth eigenmode for $V > V_{div}$ does not yield any difficulties with the number of imposed initial conditions. In polynomial eigenvalue problems, the number of roots must be equal to the number of initial conditions because, otherwise, the initial-value problem will be either overdefined or underdefined. In such problems, the continuum spectrum is absent because the poles are the only singularities of the integrand in Eq. (17). For the dynamic aeroelastic system with unsteady aerodynamics, not only initial conditions at $t = 0$ but the full history of the wing motion at $t < 0$ must be specified because the wake remembers all preceding motion that, consequently, also affects the aerodynamic loading. The resulting eigenvalue problem is not polynomial, and solution (18) of the corresponding initial-value problem has uniquely defined amplitudes of all eigenmodes (either four at $V < V_{div}$ or five at $V \geq V_{div}$) and of the continuous spectrum.

When using simplified aerodynamics, such as quasi-steady theory, aerodynamic derivatives are constants and do not have any branch cuts. Physically, this corresponds to neglecting the wake effect. Then, the continuous spectrum is absent, the eigenvalue problem is polynomial, and the number of eigenmodes is constant. In such a problem formulation, the divergence mode occurs after the interaction of an eigenmode with its paired mode, according to the classical divergence mechanism [1–3].

As well as in classical transition to divergence, from a physical point of view, the interplay of aerodynamic and structural stiffnesses is important for the divergence onset because the separation of the divergence mode from the continuous spectrum occurs when the negative aerodynamic stiffness becomes sufficiently large to make the total stiffness zero. However, in contrast to the classical mechanism, all structural eigenmodes stay damped, whereas the growing divergence mode separates from the continuous spectrum.

It is emphasized that the divergence velocity is not changed when compared to the value obtained in the steady-flow approximation because the transition occurs through $\omega = 0$, where (and only where) the steady theory is the exact solution. Hence, the new divergence mechanism does not change the stability boundary but, clearly, the analytical structure of the eigenmodes is drastically changed. This yields the practical conclusions of this study, which consist of the following. In the flight tests of flight vehicles, the crossing of the instability boundary must be avoided, and its approach should be detected in advance. Often, the tracking of structural damping and frequencies of the wing at in-flight conditions is used, and the approach of divergence is detected by the rapid decrease of the structural frequency. The results of this study show that divergence can occur without falling of the structural frequencies to zero, i.e., without any precursor in the structural mode behavior. The experimental divergence study of Ref. [23] fully confirmed this point. Hence, such dynamic indicators of the divergence approach should be used with care.

The results of the present study, where a simplistic wing and flow models were considered, are easily generalized to more sophisticated aeroelastic models, where the aerodynamic functions are not analytic on the entire complex ω plane but have branch cuts. Such models include three-dimensional subsonic compressible flow [10]. Each branch cut yields the continuous spectrum but, in general, it cannot be guaranteed that it is related with the transition to divergence. However, if the branch cut of aerodynamic functions is similar to the Theodorsen function, such as in compressible flows [10], then the transition to divergence cannot occur irrespective of the continuous spectrum because it includes $\omega = 0$. In particular, in the problem of a membrane strip in air flow [13], the transition to divergence (if analyzed through unsteady aerodynamics) occurs exactly in the same way as in the wing model considered in this study: structural eigenmodes stay damped, but the additional divergence mode separates from the continuous spectrum.

Acknowledgments

References

[1] Bisplinghoff, R. L., Ashley, H., and Halfman, R. L., *Aeroelasticity*, Addison–Wesley, Cambridge, England, U.K., 1955, Chaps. 5–7.

[2] Fung, Y. C., *An Introduction to the Theory of Aeroelasticity*, Dover, New York, 1969, Chaps. 6.7, 6.9.

[3] Wright, J. R., and Cooper, J. E., *Introduction to Aircraft Aeroelasticity and Loads*, Wiley, Chichester, England, U.K., 2015, Chaps. 9.3, 9.4, 9.6, 10.2, 10.8, 10.9.1. https://doi.org/10.1002/9781118700440

[4] Goland, M., "The Flutter of a Uniform Cantilever Wing," *Journal of Applied Mechanics*, Vol. 12, No. 4, 1945, pp. A197–A208.

[5] Theodorsen, T., "General Theory of Aerodynamic Instability and the Mechanism of Flutter," NACA Rept. 496, 1935.

[6] Sedov, L. I., "The Theory of Unsteady Gliding and Wing Motion with Running Vortices," *Proceedings of TsAGI*, No. 252, 1936 (in Russian); also Sedov, L. I., *Two-Dimensional Problems in Hydrodynamics and Aerodynamics*, Wiley, New York, 1965.

[7] *Handbook of Mathematical Functions*, Applied Mathematics Series 55, edited by M. Abramowitz, and I. A. Stegun, National Bureau of Standards, Washington, D.C., 1964, Chaps. 9.6.54, 9.6.9.

[8] Kolmogorov, A. N., and Fomin, S. V., *Elements of the Theory of Functions and Functional Analysis*, Dover, New York, 1999.

[9] Edwards, J. W., "Unsteady Aerodynamic Modeling for Arbitrary Motions," *AIAA Journal*, Vol. 17, No. 4, 1979, pp. 365–374. https://doi.org/10.2514/3.7348

[10] Stark, V. J. E., "General Equations of Motion for an Elastic Wing and Method of Solution," *AIAA Journal*, Vol. 22, No. 8, 1984, pp. 1146–1153. https://doi.org/10.2514/3.8750

[11] Case, K. M., "Stability of Inviscid Plane Couette Flow," *Physics of Fluids*, Vol. 3, No. 2, 1960, pp. 143–148. https://doi.org/10.1063/1.1706010

[12] Hassig, H. J., "An Approximate True Damping Solution of the Flutter Equation by Determinant Iteration," *AIAA Journal*, Vol. 8, No. 11, 1971, pp. 885–889. https://doi.org/10.2514/3.44311

[13] Drachinsky, A., and Raveh, D. E., "Limit-Cycle Oscillations of a Pre-Tensed Membrane Strip," *Journal of Fluids and Structures*, Vol. 60, Jan. 2016, pp. 1–22. https://doi.org/10.1016/j.jfluidstructs.2015.06.007

[14] Chen, P. C., "Damping Perturbation Method for Flutter Solution: The *g*-Method," *AIAA Journal*, Vol. 38, No. 9, 2000, pp. 1519–1524. https://doi.org/10.2514/2.1171

[15] Ju, Q., and Qin, S., "New Improved *g* Method for Flutter Solution," *Journal of Aircraft*, Vol. 46, No. 6, 2009, pp. 2184–2186. https://doi.org/10.2514/1.46328

[16] Rodden, W. P., Harder, R. L., and Bellinger, E. D., "Aeroelastic Addition to NASTRAN," NASA CR 3094, 1979.

[17] Rodden, W. P., and Bellinger, E. D., "Aerodynamic Lag Functions, Divergence, and the British Flutter Method," *Journal of Aircraft*, Vol. 19, No. 7, 1982, pp. 596–598. https://doi.org/10.2514/3.44772

[18] Rodden, W. P., and Stahl, B., "A Strip Method for Prediction of Damping in Subsonic Wind Tunnel and Flight Flutter Tests," *Journal of Aircraft*, Vol. 6, No. 1, 1969, pp. 9–17. https://doi.org/10.2514/3.43994

[19] Ueda, T., "Lifting Surface Calculations in the Laplace Domain with Application to Root Loci," *AIAA Journal*, Vol. 25, No. 5, 1987, pp. 698–704. https://doi.org/10.2514/3.9685

[20] Edwards, J. W., and Wieseman, C. D., "Flutter and Divergence Analysis Using the Generalized Aeroelastic Analysis Method," *Journal of Aircraft*, Vol. 45, No. 3, 2008, pp. 906–915. https://doi.org/10.2514/1.30078

[21] Liska, S., and Dowell, H., "Continuum Aeroelastic Model for a Folding-Wing Configuration," *AIAA Journal*, Vol. 47, No. 10, 2009, pp. 2350–2358. https://doi.org/10.2514/1.40475

[22] Vepa, R., "On the Use of Padé Approximants to Represent Unsteady Aerodynamic Loads for Arbitrarily Small Motions of Wings," AIAA Paper 1976-0017, 1976. https://doi.org/10.2514/6.1976-17

[23] Heeg, J., "Dynamic Investigation of Static Divergence: Analysis and Testing," NASA TP-2000-210310, 2000, pp. 79–80, 109–118.

[24] Daschund, D., "The Development of a Theoretical and Experimental Model for the Study of Active Suppression of Wing Flutter," Princeton Univ., Dept. of Mechanical and Aerospace Engineering TR 1596T, Princeton, NJ, Dec. 1980.

D. E. Raveh
Associate Editor